The Broad Transcription Factor Links Hormonal Signaling, Gene Expression, and Cellular Morphogenesis Events During *Drosophila* Imaginal Disc Development

Clinton Rice, Stuart J. Macdonald, Xiaochen Wang,[1] and Robert E. Ward[2,3]
Department of Molecular Biosciences, University of Kansas, Lawrence, Kansas 66045
ORCID IDs: 0000-0002-9421-002X (S.J.M.); 0000-0002-9374-2382 (R.E.W.)

ABSTRACT Imaginal disc morphogenesis during metamorphosis in *Drosophila melanogaster* provides an excellent model to uncover molecular mechanisms by which hormonal signals effect physical changes during development. The *broad* (*br*) *Z2* isoform encodes a transcription factor required for disc morphogenesis in response to 20-hydroxyecdysone, yet how it accomplishes this remains largely unknown. Here, we use functional studies of amorphic br^5 mutants and a transcriptional target approach to identify processes driven by *br* and its regulatory targets in leg imaginal discs. br^5 mutants fail to properly remodel their basal extracellular matrix (ECM) between 4 and 7 hr after puparium formation. Additionally, br^5 mutant discs do not undergo the cell shape changes necessary for leg elongation and fail to elongate normally when exposed to the protease trypsin. RNA-sequencing of wild-type and br^5 mutant leg discs identified 717 genes differentially regulated by *br*, including a large number of genes involved in glycolysis, and genes that encode proteins that interact with the ECM. RNA interference-based functional studies reveal that several of these genes are required for adult leg formation, particularly those involved in remodeling the ECM. Additionally, *br Z2* expression is abruptly shut down at the onset of metamorphosis, and expressing it beyond this time results in failure of leg development during the late prepupal and pupal stages. Taken together, our results suggest that *br Z2* is required to drive ECM remodeling, change cell shape, and maintain metabolic activity through the midprepupal stage, but must be switched off to allow expression of pupation genes.

KEYWORDS morphogenesis; ecdysone; *Drosophila melanogaster* metamorphosis; imaginal disc development

TISSUE morphogenesis is required for the elaboration of the body axis and organs during metazoan development. In some contexts, hormonal signals provide temporal cues to coordinate these morphogenetic events. Imaginal disc morphogenesis in the fruit fly *Drosophila melanogaster* provides an excellent model to uncover molecular mechanisms by which hormonal signals are translated into the physical changes that occur during development. Imaginal discs are diploid tissues found within the larva that give rise to the adult integument during metamorphosis (Willis 1974; Csaba 1977; Fristrom 1988). Both classical experiments and more recent live imaging studies (De las Heras *et al.* 2018; Diaz-de-la-Loza *et al.* 2018) have revealed requirements for cell shape changes and rearrangements, as well as for remodeling of the extracellular matrix (ECM) in imaginal disc morphogenesis during metamorphosis. These experiments also demonstrate the key role that 20-hydroxyecdysone (hereafter referred to as ecdysone) plays in directing these processes. Ecdysone acts through a transcriptional cascade: the hormone binds to its heterodimeric receptor, which acts as a DNA-binding activator to drive transcription of early-response genes, including *Eip74EF*, *Eip75B*, and *broad* (*br*), which themselves encode DNA-binding proteins that activate late-response genes (Chao and Guild 1986; Feigl *et al.* 1989; Janknecht *et al.* 1989; Burtis *et al.* 1990; Segraves and

doi: https://doi.org/10.1534/genetics.120.303717
Manuscript received January 22, 2020; accepted for publication October 5, 2020; published Early Online October 28, 2020.
Supplemental material available at figshare: https://doi.org/10.25386/genetics.11729019.
[1]Present address: State Key Laboratory of Experimental Hematology, Institute of Hematology and Blood Diseases Hospital, Chinese Academy of Medical Sciences, Tianjin, China.
[2]Present address Department of Biology, Case Western Reserve University, Cleveland, Ohio 44106.
[3]Corresponding author: Department of Biology, Case Western Reserve University, 2080 Adelbert Road, Cleveland, OH 44106. E-mail: rew130@case.edu

Hogness 1990; DiBello *et al.* 1991; Yao *et al.* 1993; Crossgrove *et al.* 1996). Despite extensive research into *Drosophila* metamorphosis, parts of the pathway connecting the ecdysone cue to the effectors involved in imaginal disc morphogenesis have yet to be elucidated.

Of the ecdysone signaling early-response genes, *br* appears to have the most direct effects on imaginal disc morphogenesis (Kiss *et al.* 1988). *br* encodes four transcription factors, each carrying a unique zinc finger domain spliced to a common Broad-Complex, Tramtrack, and Bric a Brac/Pox virus and Zinc finger (BTB/POZ) domain (DiBello *et al.* 1991; von Kalm *et al.* 1994; Bayer *et al.* 1996) (Supplemental Material, Figure S1). These four isoforms, known as the Z1, Z2, Z3, and Z4 isoforms, have three genetically separate functions (*br*, *reduced bristles on the palpus*, and *2Bc*), with the Z2 isoform performing the classic *br* function (Bayer *et al.* 1997). This function is critical for imaginal disc morphogenesis: animals lacking functional Br Z2 have discs that fail to elongate, and these animals die during the prepupal stage before head eversion (Kiss *et al.* 1988). The various isoforms of Br also add a layer of complexity to the regulation of metamorphic genes. *br* does not simply respond to the ecdysone cue through a general increase in transcription that subsequently effects the increased transcription of late-response genes; rather, the isoforms exhibit a dynamic pattern of expression that differs by tissue (Huet *et al.* 1993). In the imaginal discs, the expression of the Z2 transcript rises dramatically approximately 4 hr before pupariation, but greatly decreases in the hours after pupariation, while the expression of the Z1 transcript greatly increases between 2 and 4 hr after pupariation (Emery *et al.* 1994; Bayer *et al.* 1996). This late larval pulse of Z2 expression is critical for activation of late-response genes; however, the identities of these genes remain largely unknown. The illumination of the link between the ecdysone cue and morphogenetic effects in imaginal discs hinges upon the identification of these late-response genes and how they are regulated by ecdysone and *br*.

Previous screens using the hypomorphic br^1 allele identified a number of *br*-interacting genes, including *Stubble* (*Sb*), *zipper*, *Rho1*, *Tropomyosin 1*, *blistered*, and *ImpE3* (Beaton *et al.* 1988; Ward *et al.* 2003), although the majority of these genes are not transcriptional targets of *br* (Ward *et al.* 2003). Nevertheless, the identity of these genes suggests roles for *br* in the major processes implicated in hormonal control of imaginal disc morphogenesis, namely cell shape changes/rearrangements and modification of the ECM. Here, we show that cell shape changes and cell rearrangements fail to occur normally in br^5 mutant prepupae. In addition, consistent with previous work demonstrating that the ECM provides a constraining force and must be degraded to allow disc elongation (Pastor-Pareja and Xu 2011; Diaz-de-la-Loza *et al.* 2018), we show that the basal ECM protein Collagen IV is not substantially degraded in leg imaginal discs from amorphic br^5 mutant animals as old as 8 hr after puparium formation (APF). In this study, we also use this allele to identify specific genes regulated by *br* in the leg discs at the onset of metamorphosis through an RNA-sequencing-based approach. This approach identified over 700 *br*-regulated genes, including genes with known metabolic and developmental functions, including ECM organization and modification. We tested a subset of these genes for roles in leg morphogenesis through RNA interference (RNAi) and found several that are necessary for proper development of the adult legs. These results demonstrate the value of a transcriptional target-based approach to identifying morphogenetic genes, and suggest that *br* regulates morphogenesis through the regulation of genes involved in multiple critical processes.

Materials and Methods

Fly stocks

All *Drosophila* stocks were maintained on media consisting of corn meal, sugar, yeast, and agar in incubators maintained at a constant temperature of 25° or at room temperature. w^{1118}, ybr^5, br^1, *distalless* (*dll*)-*Gal4*, *apterous* (*ap*)-*Gal4*, *P{UAS-Dcr-2.D}1*, w^{1118}, $Pgm1^{LA00593}$, and the Transgenic RNAi Project lines ("short-hairpin" RNAi lines; https://fgr.hms.harvard.edu) were obtained from the Bloomington *Drosophila* Stock Center (Bloomington, IN). "Long-hairpin" RNAi lines were obtained from the Vienna *Drosophila* RNAi Center (Vienna, Austria; Dietzl *et al.* 2007). *UAS-serp* was obtained from Stefan Luschnig (University of Muster). *UAS-Verm/CyO* was obtained from Christos Samakovlis (Stockholm University). *vkg-GFP* (Flytrap; Buszczak *et al.* 2007) was obtained from Sally Horne-Badovinac (University of Chicago). *w*; *hs-Z2 (CD5-4C)*; *hs-Z2 (CD5-1)* was obtained from Cindy Bayer (University of Central Florida). *Loxl-1-RNAi* (stock 11335R) was obtained from the National Institutes of Genetics Fly stock collection (Kyoto, Japan). *dll-Gal4* was balanced with *CyO*, *P{w+, Dfd-EYFP}* (Le *et al.* 2006). w^{1118} was used as the wild-type control, unless otherwise noted. All fly stocks and reagents are listed and described in the reagents table.

br isoforms

To clarify the relationship between the isoforms of the *br* gene listed on FlyBase and the Br protein isoforms bearing the Z1, Z2, Z3, and Z4 zinc finger domains, translated sequences of all 15 *br* isoforms listed on FlyBase were downloaded from FlyBase and aligned using Clustal Omega (Goujon *et al.* 2010; Sievers *et al.* 2011; Thurmond *et al.* 2019). The first 431 amino acids represent the Br "core" region and were shared among all isoforms; the remaining amino acids were compared to the published Z1, Z2, Z3, and Z4 zinc finger domain sequences to determine which zinc finger was carried by each FlyBase isoform (DiBello *et al.* 1991; Bayer *et al.* 1996).

Fly staging, dissection, and photography of live leg imaginal discs

w^{1118} and ybr^5/*Binsn* flies were staged on food supplemented with 0.05% bromophenol blue, as described in Andres and Thummel (1994). w^{1118} and ybr^5/*Y* mutant animals were

selected (mutant males were selected using the *yellow* marker) at −18 hr (blue gut larvae), −4 hr (white gut larvae), 0 hr (white prepupae), and +2 hr and +4 hr relative to puparium formation. Leg imaginal discs were dissected in phosphate-buffered saline (PBS), and then transferred to fresh PBS. Brightfield photomicrographs were captured within 5 min on a Nikon Eclipse 80i microscope equipped with a Photometrics CoolSNAP ES high performance digital CCD camera using a Plan APO ×10 (0.45 NA) objective. For the examination of collagen integrity in prepupal leg discs, we crossed *ybr^5/Binsn* virgins to *w^{1118}*, *vkg-GFP* males, and crossed F_1 *ybr^5/w^{1118}*; *vkg-GFP/+* females to *w^{1118}* males. We selected *ybr^5/Y*; *vkg-GFP/+* and *w^{1118}/Y*; *vkg-GFP/+* white prepupae based upon the *y* phenotype and aged them at 25°. *ybr^5* prepupae were confirmed to contain the *br^5* allele based upon pupal morphology. We dissected leg imaginal discs at the indicate time points in PBS, mounted them live in mounting media (90% glycerol, 100 mM Tris pH 8.0, 0.5% n-propyl-gallate) and imaged them sequentially with brightfield microscopy and wide-field fluorescence microscopy on a Nikon Eclipse 80i microscope equipped with a Photometrics CoolSNAP ES high performance digital CCD camera, using a Plan APO ×20 (0.75 NA) objective. All images were captured with identical settings (light or fluorescence intensities, and exposure times). On average, three or four discs were imaged from each prepupa, and at least seven different prepupae were imaged at each time point. All digital images were cropped and adjusted for brightness and contrast in Adobe Photoshop (version CC 2018; Adobe, San Jose, CA) or ImageJ (version 1.51r; National Institutes of Health, Bethesda, MD), and figures were compiled using Adobe Illustrator (version CC 2018).

Trypsin experiments

w^{1118} and *br^5* white prepupae were dissected in PBS to isolate three leg imaginal discs from the same animal. These imaginal discs were incubated on 3-well depression slides in either PBS, PBS plus 0.025% trypsin (25200-056; Gibco) or PBS plus 0.0025% trypsin for 15 min at room temperature, at which point they were immediately imaged by brightfield microscopy on a Nikon Eclipse 80i microscope equipped with a Photometrics CoolSNAP ES high performance digital CCD camera using a Plan APO ×10 (0.45 NA) objective. In total, 21 *w^{1118}* and 17 *br^5* animals were dissected and imaged.

Immunostaining

Imaginal discs were hand dissected from *w^{1118}* or *br^5* +4 hr prepupae in fresh PBS, and fixed immediately in 4% paraformaldehyde for 20 min. The following antibodies were used at the given dilutions: rat anti-DE-cadherin (clone DCAD2 from Developmental Studies Hybridoma Bank at the University of Iowa) at 1:25, rabbit anti-Vermiform (gift from Stefan Luschnig, University of Munster) at 1:1000 (Luschnig *et al.* 2006), Donkey anti-rabbit Cy3 (Jackson ImmunoResearch Laboratories, West Grove, PA) at 1:400 and donkey anti-rat Cy2 (Jackson ImmunoResearch Laboratories) at 1:400. Confocal images were acquired on a Leica SPE laser scanning confocal microscope using an ACS APO ×40 (1.15 NA) oil immersion lens. All digital images were cropped and adjusted for brightness and contrast in ImageJ (version 1.51s; National Institutes of Health). Figures were compiled using Adobe Illustrator (version CC 2018).

RNA-sequencing and data analysis

To control for potential genetic effects from the autosomes and Y chromosome, we crossed *ybr^5/Binsn* females to *w^{1118}* males and then crossed the resulting *ybr^5/w^{1118}* females with *w^{1118}* males. This cross produced *ybr^5/Y* and *w^{1118}/Y* males that, at a population level, had identical autosomes and Y chromosomes. Since we selected the *br^5* animals based upon the *yellow* cuticular phenotypes, we tested to make sure that *y* and *br* did not recombine apart to any significant degree. *y* and *br* are reported to map 0.2 cM apart on the X chromosome (Gatti and Baker 1989), and in two separate experiments we did not detect any recombination between these genes ($n > 200$). After RNA-sequencing, we identified the *br^5* mutation as a C to T transition at position 1654571 in GenBank AE014298 (X chromosome of *D. melanogaster*), converting a conserved histidine in the zinc finger of the Z2 isoform into a tyrosine. We found that all the reads through this interval had the mutation in the *br^5* samples, whereas none of the reads from *w^{1118}* samples had the mutation.

Third instar *ybr^5/Y* and *w^{1118}/Y* larvae were staged on food supplemented with 0.05% bromophenol blue. Blue gut larvae (−18 hr) and white prepupae (0 hr) were selected and leg imaginal discs were hand-dissected in PBS. Triplicate independent samples were obtained for *ybr^5/Y* and *w^{1118}/Y* white prepupae and for *w^{1118}/Y* −18 hr larvae. Total RNA was isolated using TriPure (Roche, Indianapolis, IN) and then purified over RNAeasy columns (Qiagen, Valencia, CA). Approximately 5 μg of total purified RNA was obtained for each sample, and ∼1 μg of each sample was provided to the Genome Sequencing Core at the University of Kansas for library preparation using the TruSeq stranded mRNA kit (Illumina, San Diego, CA). Single read 100 (SR100) was performed on a single lane of an Illumina HiSeq 2500 (Genome Sequencing Core, University of Kansas).

The quality of the raw RNA-sequencing reads was visually confirmed using FastQC (version 0.11.5; Andrews 2010), and both low-quality data and adaptor sequences were removed using Trimmomatic (version 0.36; Bolger *et al.* 2014). The number of remaining reads per sample averaged 18.1 million (range = 12.6–22.8), and all reads were at least 50-nt in length. Filtered reads were mapped to the *D. melanogaster* reference genome (Release 5.3) using TopHat (version 2.1.1; Trapnell *et al.* 2009; Kim *et al.* 2013). Default parameters were employed, with the addition of the "–no-novel-juncs" flag to use the gene annotation as provided, and the "–library-type fr-firststrand" flag since the RNA-sequencing data derives from the Illumina TruSeq stranded mRNA kit. On average 86.2% of the reads mapped to the reference across samples (range = 83.1–88.5). Genotypes were compared,

and differentially-expressed genes were identified using the Cufflinks pipeline (version 2.2.1; Trapnell *et al.* 2010; Roberts *et al.* 2011; Trapnell *et al.* 2013). Specifically, we employed the "cuffquant" and "cuffdiff" routines using default parameters, adding the "-b" flag to run a bias correction algorithm that improves expression estimates (Roberts *et al.* 2011).

Bioinformatic analyses

Gene ontology analysis was performed using the Gene Ontology Consortium's (http://www.geneontology.org) gene ontology enrichment analysis tool (Gene Ontology Consortium 2015). To ensure we were considering genes showing large-scale induction or repression, significantly differentially expressed genes showing ≥1.5-fold change between w^{1118} 0 hr and br^5 0 hr samples and at least 5 fragments per kilobase of exon per million fragments mapped (FPKM) in the sample showing higher expression (w^{1118} for *br*-induced genes, br^5 for *br*-repressed genes) were used as input into the tool. In a second experiment, significantly differentially expressed genes showing ≥1.5-fold change between w^{1118} –18 and 0 hr samples and at least 5 FPKM in the sample showing higher expression (w^{1118} 0 hr for developmentally induced genes and w^{1118} –18 hr for developmentally repressed genes) were used. The same data sets were used for the Kyoto Encyclopedia of Genes and Genomes (KEGG) pathway analysis using WebGestalt's (http://www.webgestalt.org) overrepresentation analysis (Wang *et al.* 2017).

ATP measurement

Leg and wing imaginal discs were dissected from +4 hr w^{1118} and br^5 mutant prepupae in PBS and immediately homogenized in 100 μl of lysis buffer (6 M guanidine HCl, 100 mM Tris pH 7.8, 4 mM EDTA) on ice and frozen. A mixed leg and wing sample was used in this experiment to allow all of the dissections to be completed in one sitting with enough material for the subsequent analysis. We note that prior Northern blot analysis using a mixed sample of leg and wing imaginal disc material showed identical expression of ecdysone and Rho signaling pathway gene expression to those composed only of leg imaginal disc material, and that wing discs arrest development in br^5 prepupa at the same stage that leg discs do (R. Ward, unpublished data). After all of the samples were collected, they were thawed to 4°, and a 10 μl aliquot was taken for protein measurement using a Bradford Assay (Bio-Rad, Hercules, CA). The remaining sample was boiled for 5 min, spun at 13,000 rpm in a refrigerated microcentrifuge for 3 min, and then 10 μl of the supernatant was diluted into 90 μl of dilution buffer (25 mM Tris pH 7.8, 100 μM EDTA). This sample was further diluted 10-fold in dilution buffer and 10 μl of this sample was used for ATP quantification using the ATP Determination Kit (A22066; Molecular Probes, Eugene, OR) according to the manufacturer's protocol, using a BioTek Synergy HT plate reader. Each biological sample contained ∼13 wing discs and 35 leg discs. Triplicate samples were processed and three technical replicates of each biological sample was assayed, along with a dilution series of ATP from 1 nM to 1 μM. Statistical analysis was performed using a type 3 ANOVA with protein level and treatment as factors.

Northern blot analysis

Progeny from a cross of $ybr^5/Binsn$ X *Binsn/Y* were staged on standard *Drosophila* media supplemented with 0.05% bromophenol blue, as described in Andres and Thummel (1994). Total RNA was isolated by direct phenol extraction from leg imaginal discs dissected from staged *Binsn/Y* males. Approximately 9 μg of total RNA per sample were separated by formaldehyde agarose gel electrophoresis and transferred to a nylon membrane. The membrane was hybridized and stripped as described in Karim and Thummel (1991). Generation of probe fragments for *br* (*br* core and *br-Z2*) and *rp49* is described in Andres and Thummel (1994). Specific probes were labeled by random priming of gel-purified fragments (Stratagene, St. Louis, MO).

Functional analyses

To amplify potential RNAi in long-hairpin lines, we crossed a *UAS-Dicer* transgene onto the *Gal4* lines used to drive the expression of the gene-specific double-stranded RNA to produce *P{UAS-Dcr-2.D}1*, w^{1118}; *Dll-GAL4/CyO*, *dfd-YFP* and *P{UAS-Dcr-2.D}1*, w^{1118}; *ap-GAL4/CyO*, *dfd-YFP*. For consistency, we also used these recombined lines when crossing to short-hairpin RNAi lines. Virgin females of these genotypes were then mated to *UAS-RNAi* males. The vials were kept in incubators maintained at a constant temperature of 25°. The adults were transferred twice to new vials, and newly eclosing F_1 flies were separated by phenotype and examined for malformed third legs each day for a total of 8 days per vial. We considered an animal to be malformed if it displayed malformation in at least one leg, and defined a leg as malformed if any femur, tibia, or tarsal segment was bent, twisted, missing, or was excessively short and fat.

To control for background effects that may contribute to the appearance of malformed legs, we crossed *UAS-Dcr1*, w^{1118}; *Dll-GAL4/CyO*, *dfd-YFP* virgin females with males from the w^{1118} line and a *loxl1*-RNAi line and examined the offspring for malformed legs. Curly-winged offspring from RNAi crosses, which carry the *UAS-RNAi* hairpin construct, but not the GAL4 driver, were also examined. A few of the RNAi constructs were carried over a balancer chromosome; only flies without the balancer were counted. Flies carrying malformed legs did not exceed 1% of all flies in either control cross, and exceeded 1% among curly-winged offspring from only two RNAi crosses. In neither of these two crosses (carrying RNAi hairpin constructs against *CG7447* and *E[spl]m4*) did flies carrying malformed legs exceed 2% of all curly-winged flies, and neither of these crosses were among those in which a significant number of straight-winged flies carried malformed legs. For crosses in which we examined preadult

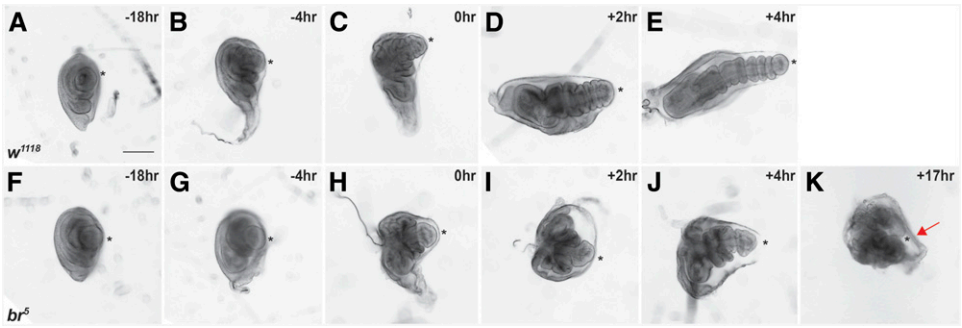

Figure 1 *Broad* is required for normal prepupal leg imaginal disc development. Brightfield photomicrographs of leg imaginal discs from w^{1118} (A–E) and br^5 (F–K) mutant larvae and prepupae. Times given are relative to puparium formation. Note that leg imaginal discs are similar between w^{1118} and br^5 during larval time points (−18 and −4 hr), but are noticeably different starting at 0 hr. Although w^{1118} discs elongate from the center (distal tarsal segment; indicated by asterisk) and are segmented by +4 hr, br^5 discs show limited elongation and have wider tarsal segments. Intact leg imaginal discs can be found inside dead br^5 prepupae as late as 17 hr after pupariation. These late imaginal discs have not elongated much past the +4 stage and often have an intact peripodial epithelium (arrow). Bar, 100 μm.

stages expressing RNAi, individuals carrying the *Dll-GAL4* driver were identified by the lack of *dfd-YFP* expression.

br-Z2 overexpression studies

Approximately 50 *HS-br-Z2* or w^{1118} late larvae were placed into an empty fly vial with a piece of moist Whatman paper in the bottom of the vial. The vial was heat shocked in a 37° incubator for 60 min, after which any animals that had pupariated were removed. The vial was moved to a 25° incubator for 6 additional hours, at which point all prepupae were removed to a food vial for further development (also at 25°). After a further 18 hr, the prepupae were scored to determine if they had pupated. The animals were then left at 25° and scored for eclosing 4 days later. In some experiments, *HS-br-Z2* or w^{1118} were collected as they pupariated, aged 4 hr at 25°, and dissected to examine their leg imaginal discs. Another subset was dissected at approximately 16 hr after pupariating to examine the terminal leg imaginal disc phenotypes. All dissections, microscopy, and image preparation were conducted as described above.

Adult specimen preparations

Adult legs were dissected from the third thoracic segment in PBS, cleared in 10% KOH overnight, and mounted in Euparal (Bioquip, Gardena, CA) on microscope slides. Images of adult leg cuticles were captured on a Photometrics CoolSNAP ES high performance digital CCD camera with a Nikon Eclipse 80i microscope. All digital images were cropped and adjusted for brightness and contrast in ImageJ (version 1.51r; National Institutes of Health) and figures were compiled using Adobe Illustrator (version CC 2018).

Data availability

Fly stocks are available upon request. Figure S1shows the gene structure and RNA isoforms of the *broad* locus. Figure S2 shows the results of luciferase ATP assays to quantify ATP levels between w^{1118} and br^5 +4 hr leg discs. Figure S3 compares +4 hr leg imaginal discs from w^{1118}, br^5, and *Dll* > *br-RNAi*-expressing animals. Table S1 shows the genes that are differentially expressed between w^{1118} and br^5 0 hr leg discs. Table S2 shows the gene ontology terms that are significantly over- and underrepresented in the *br*-induced and *br*-repressed gene sets. Table S3 shows the KEGG pathway analyses on the *br*-induced and br-repressed gene sets. Table S4 shows the genes that are differentially expressed between −18 and 0 hr in w^{1118} leg discs. Table S5 shows the gene ontology terms that are significantly over- and underrepresented in the w^{1118} developmentally regulated gene sets. The reagents table lists all the stocks and reagents used in this study. All RNA-sequencing data sets are available from the Gene Expression Omnibus. The project accession number is GSE140248, and the project title is "Genome-wide differences in RNA expression in *Drosophila melanogaster* leg imaginal discs based on time and presence/absence of broad-based gene regulation." Supplemental material available at figshare: https://doi.org/10.25386/genetics.11729019.

Results

Phenotypic characterization of br^5 mutant leg imaginal discs

To identify genes regulated by *br* during metamorphosis using an RNA-sequencing approach, we wanted to use a null *br* allele. The br^5 allele has been reported to be amorphic, with homozygous mutants failing to develop past the early prepupal stage (Kiss *et al.* 1988). Consistent with this notion, br^5 encodes a protein with a His^{492}–Tyr substitution in the conserved Z2 zinc finger domain, suggesting that it has defective DNA binding properties (L. von Kalm, personal communication; confirmed in the RNA-sequencing; see *Materials and Methods*). We previously used live imaging to show that br^5 hemizygous mutants failed to complete metamorphosis (Ward *et al.* 2003). To more closely examine how imaginal disc development is disrupted in these animals, we dissected and compared leg discs from br^5 and w^{1118} larvae and prepupae (Figure 1). br^5 leg discs resemble w^{1118} leg discs during larval stages (through 4 hr before pupariation), consisting of a columnar epithelium with folds that make three to four concentric circles. The discs bulge from the central circles (which develop into the distal-most leg segments), and are

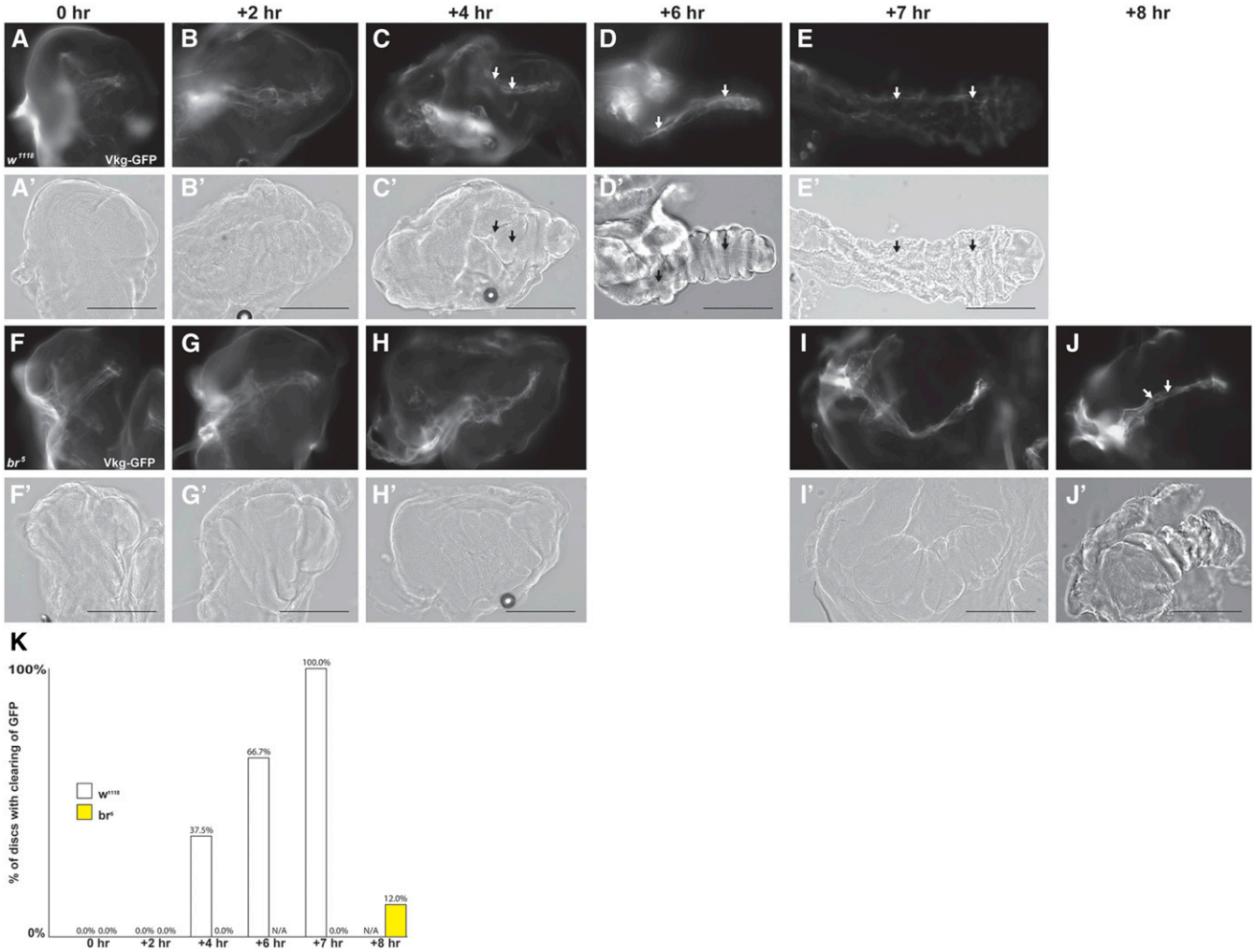

Figure 2 *broad* is required for efficient degradation of the basal ECM in prepupal leg imaginal discs. Wide-field fluorescence (A–J) and brightfield (A′–J′) photomicrographs (at the same focal plane) of leg imaginal discs from w^{1118} (A–E) and br^5 mutant (F–J) prepupae expressing Viking-GFP (Collagen IV). Ages of the animals relative to puparium formation are indicated above the figures. Note that Viking-GFP forms cables of ECM lining the lumen at the basal side of elongating leg discs, which are gradually cleared from +4 to +7 hr APF in w^{1118} leg discs (white arrows in C, D, E, and J; black arrows in C′, D′, E′, and J′ represent matching location in brightfield images). Similar clearing is not observed in the br^5 mutant discs and persists at least through 8 hr APF (J) in many animals. Bar, 100 μm. (K) Graph showing percentage of discs showing partial or total clearing of GFP expression in the channel.

covered by the peripodial epithelium. By the prepupal stage, leg discs begin to differ between the two genotypes. Both br^5 and w^{1118} discs begin to elongate in a telescoping fashion at the onset of metamorphosis (0 hr), beginning with the centermost regions. However, by 2 hr after pupariation, elongation of br^5 discs clearly lags behind that of w^{1118} discs. w^{1118} discs continue to elongate and by 4 hr after pupariation, the future five tarsal segments and distal tibia are clearly identifiable underneath the peripodial epithelium. br^5 mutant discs, on the other hand, form shorter, wider structures with deeper folds between the tarsal segments. br^5 mutant discs show only limited elongation over subsequent hours and fail to evert to the outside of the prepupa. This phenotype is completely penetrant ($n > 1000$ leg discs examined). Notably, imaginal discs can be found inside degenerating br^5 mutant late prepupae that look similar to +4 hr mutant discs, including having an intact peripodial epithelium ($n > 20$ animals; Figure 1K).

The disruption of prepupal elongation in br^5 mutants, coupled with the presence of the peripodial epithelium in late-staged prepupae (which is known to be degraded by matrix metalloproteinases; Proag *et al.* 2019), motivated us to examine ECM breakdown in wild-type and br^5 mutant discs. We therefore crossed a GFP-tagged version of Collagen IV (Vkg-GFP) into w^{1118} and br^5 and examined their leg discs at various time points during metamorphosis (Figure 2). At early stages (0 and 2 hr after pupariation), wild-type and br^5 leg discs closely resemble one another, with fibrous cylindrical or nearly conical basal ECM structures. By 4 hr after pupariation, some wild-type discs exhibit degradation of the basal ECM. This degradation takes the form of a "clearing" of a central channel along the length of the disc. In total, 37.5%

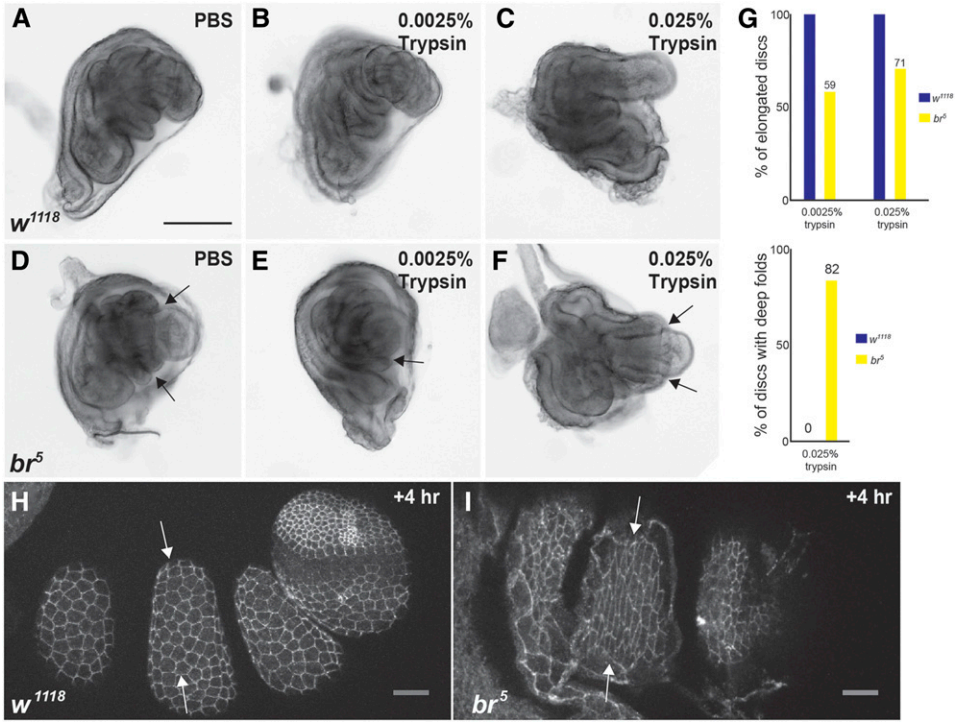

Figure 3 br^5 leg discs show aberrant elongation upon application of trypsin, and retain anisometric cell shapes through 4 hr after pupariation. (A–F) Brightfield photomicrographs of leg imaginal discs from a representative w^{1118} (A–C) and br^5 (D–F) mutant 0 hr prepupa incubated for 15 min in PBS (A and D) or 0.0025% trypsin (B and E) or 0.025% trypsin (C and F). All three discs are from the same animal. The w^{1118} discs elongate in the lower dose of trypsin, and elongate more in the higher dose of trypsin to the point where the segmental folds are pulled smooth. In contrast, br^5 mutant discs show less elongation in trypsin overall, and deeper folds in the presumptive tarsal segments (arrows). (G) Quantification of the elongation defects and aberrantly folded leg discs from w^{1118} and br^5 mutant prepupae. (H and I) Confocal optical sections of tarsal segments from leg imaginal discs from w^{1118} (H) and br^5 (I) mutant +4 hr leg imaginal discs stained with antibodies against DE-Cadherin (distal tarsal segments are to the right in each image). Note that in the w^{1118} discs, epithelial cells in the tarsal segments are mostly isometric, whereas cells in the br^5 tarsal segments are anisometric with longer circumferential cell lengths (arrows). Bar, 100 μm.

of wild-type discs (n = 32, from 12 animals) showed this clearing at 4 hr after pupariation, 66.7% (n = 21, from 12 animals) at 6 hr, and 100% (n = 12, from 8 animals) at 7 hr (Figure 2K). In contrast, most br^5 mutant discs retained the fibrous ECM appearance as late as 8 hr after pupariation (Figure 2, J and K). Only 12.0% of discs (n = 25, from 7 animals) showed partial clearing; the other discs showed no clearing.

Since br^5 mutant leg imaginal discs show reduced elongation and defective proteolysis of the ECM, we wondered whether an exogenous protease could restore normal elongation to the br^5 discs. We therefore dissected three leg imaginal discs from individual w^{1118} or br^5 animals at the onset of metamorphosis and treated one with 0% trypsin (PBS control), another with 0.0025% trypsin, and the third with 0.025% trypsin for 15 min at room temperature. Leg imaginal discs from 18 of the 21 w^{1118} animals had clearly elongated after 15 min in 0.0025% trypsin (Figure 3B). The tarsal segments in these discs were still obviously segmented, although in some cases the depth of the folds at these segment boundaries was reduced relative to the PBS control discs. w^{1118} leg discs incubated for 15 min in 0.025% trypsin showed even greater elongation (in 100% of the discs), but only with noticeable tarsal segment boundaries in two of the discs, whereas the remainder had elongated discs with the tarsal segments appearing as one long continuous segment (Figure 3C). In the br^5 mutant leg discs, there was a clear difference in the morphology of the leg discs at the onset of the experiment (which remained unchanged through 15 min in PBS; data not shown) compared to the w^{1118} discs, in which the distal tarsal segment was rounder and the folds between the tarsal segments were noticeably deeper (Figure 3D *vs.* Figure 3A). A total of 10 of the 17 discs treated with 0.0025% trypsin showed some elongation of the tarsal segments, but no shallowing of the segment boundaries (Figure 3, E and G). Similarly, 12 of the 17 discs treated with 0.025% trypsin showed an increase in the degree of elongation (Figure 3G). The morphology of these discs was clearly distinct from w^{1118} treated similarly. The absolute level of elongation in br^5 was less than in w^{1118}, and more interestingly, the br^5 discs did not eliminate the folds between segments, but rather deepened those folds (Figure 3F). This morphology was observed in 14 of the 17 discs examined (Figure 3G).

Given that trypsin was not able to elongate br^5 leg discs to the extent of that observed in w^{1118} discs, and that br^5 discs display aberrant morphology as early as the onset of metamorphosis, we suspected that the underlying cell shape changes and/or rearrangements that normally occur in wild-type animals do not occur in these mutant animals. To address this question, we examined cell shapes in the distal tarsal segments of +4 hr prepupal leg imaginal discs from w^{1118} and br^5 mutant animals using antibodies against DE-Cadherin. Although epidermal cells from w^{1118} +4 hr leg discs are generally isometric, being equally long in the

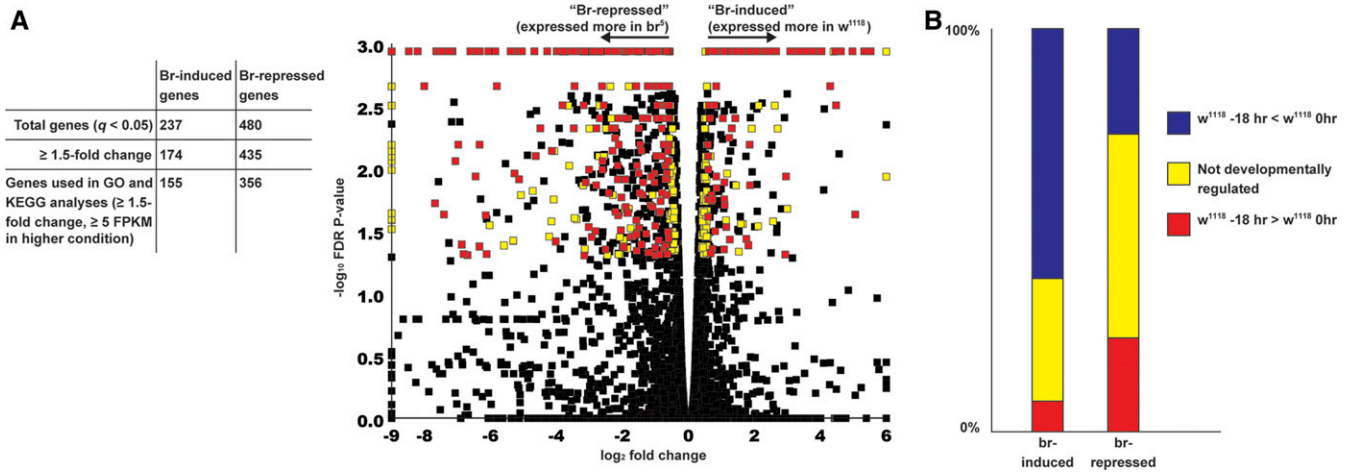

Figure 4 Over 700 genes are significantly differentially expressed in the absence of functional *br-Z2*. (A) Volcano plot of genes differentially regulated in br^5 mutant leg imaginal discs relative to w^{1118} controls. Red denotes genes with large-scale induction or repression that were used in the gene ontology and KEGG analyses, while yellow denotes genes that were significantly differentially regulated but not included in the analyses (fold change <1.5 or FPKM <5). (B) Overlap of *br*-regulated genes with developmentally regulated genes. Most *br*-induced genes were developmentally upregulated (62.0% were higher in 0 hr w^{1118} prepupae than in −18 hr w^{1118} larvae; only 7.6% were significantly higher at −18 hr), while a comparatively smaller portion of the *br*-repressed genes were developmentally downregulated (23.3%, compared to 26.3% that were developmentally upregulated).

proximal-distal and circumferential dimensions (Figure 3H), epidermal cells from br^5 +4 hr leg discs show considerable anisometry, with longer cell dimensions in the circumferential axis than the proximal-distal axis (Figure 3I). This phenotype is completely penetrant (based upon five experiments with leg discs from >30 mutant animals). The br^5 mutant distal tarsal segments are also wider at +4 hr than w^{1118} leg discs (Figure 1E *vs.* Figure 1J), suggesting a defect in cell rearrangements that are known to occur in wild type (Condic *et al.* 1991), although the defect in segmentation in the br^5 discs make this difficult to quantify.

Identification and bioinformatic characterization of genes regulated by br in prepupal leg discs

To better understand the role of *broad* in regulating imaginal leg morphogenesis, we used RNA-sequencing to identify genes that are differentially expressed between w^{1118} and br^5. We dissected leg discs from these animals at the onset of metamorphosis (0 hr), the time we first see differences in the tissues between genotypes. We generated libraries from three biological replicates per genotype and sequenced them on an Illumina HiSeq 2500. We then mapped reads to the reference genome (release 5.3) with TopHat, and used the Cufflinks pipeline to identify a total of 717 genes that were significantly differentially expressed between the two genotypes (at a false discovery rate of 5%) (Figure 4) (Trapnell *et al.* 2009; Trapnell *et al.* 2010; Roberts *et al.* 2011; Kim *et al.* 2013; Trapnell *et al.* 2013). About two-thirds of these genes (66.9%) were more highly expressed in the br^5 genotype. We refer to these genes as *br*-repressed genes (and genes that were more expressed in w^{1118} as *br*-induced genes).

To investigate which functions might be regulated by *br*, we identified gene ontology terms that were significantly overrepresented in our data sets using the Gene Ontology Consortium's gene ontology enrichment analysis tool (Gene Ontology Consortium 2015) (Table S1). To ensure we were considering genes showing large-scale induction or repression, we used *br*-induced and *br*-repressed genes with fold changes ≥1.5 and FPKM ≥5 in at least one of the samples, leaving 155 *br*-induced genes and 356 *br*-repressed genes. Significantly overrepresented gene ontology terms for this set of genes included "Notch signaling," "Molting cycle, chitin-based cuticle," and "Developmental process". Metabolic gene ontology terms for this set of genes included "glycolytic process," "glycogen metabolic process," and "carbohydrate biosynthetic process" (Table 1 and Table S2). KEGG pathway analysis of the same set of genes using WebGestalt (Wang *et al.* 2017) revealed significant overrepresentation of genes involved in glycolysis/gluconeogenesis, and several sugar metabolism pathways for *br*-induced genes (Table S3). Many *br*-induced genes have predicted cell signaling, developmental, or metabolic functions.

Since *br* serves as an early-response gene to the late larval ecdysone pulse (Chao and Guild 1986; DiBello *et al.* 1991), we expected that *br*-regulated genes would essentially represent a subset of genes regulated by ecdysone. To test this idea, we conducted a second set of RNA-sequencing analyses comparing genes expressed in mid-third instar (−18 hr) w^{1118} leg imaginal discs to those expressed in w^{1118} leg imaginal discs at the onset of metamorphosis (0 hr). A total of 1186 genes are significantly upregulated at the 0 hr stage relative to the −18 hr stage (developmentally induced genes), while 1193 genes are significantly downregulated (developmentally repressed genes) (Table S4). We anticipated that these developmentally regulated genes would serve as a proxy for ecdysone-regulated genes; consistent with this expectation, many known ecdysone-regulated genes are found in this data set, including *Eip74EF*, *E23*,

Table 1 Selected significantly enriched biological process GO terms for *br*-induced genes

GO term	No. of genes	Expected	Fold change	Significance
Single-organism carbohydrate catabolic process	9	0.27	32.93	3.91E-08
ATP generation from ADP	8	0.23	35.37	3.14E-07
Glycolytic process	8	0.23	35.37	3.14E-07
ADP metabolic process	8	0.25	32.65	5.86E-07
Pyruvate metabolic process	8	0.33	24.25	5.88E-06
Notch signaling pathway	8	0.52	15.43	1.87E-04
Molting cycle, chitin-based cuticle	8	0.91	8.75	1.26E-02
Developmental process	55	31.49	1.75	1.39E-02
Anatomical structure development	53	30.32	1.75	2.30E-02
Organ morphogenesis	22	7.98	2.76	4.11E-02

Shown above are selected gene ontology (GO) terms representative of those found to be significantly overrepresented among *br*-induced genes. See Table S2 for the full list.

and *Cyp18a1* (Janknecht *et al.* 1989; Burtis *et al.* 1990; Hurban and Thummel 1993; Bassett *et al.* 1997; Hock *et al.* 2000). Significantly enriched gene ontology terms in the developmentally induced genes include numerous terms related to developmental processes, such as "imaginal disc eversion" and "regulation of tube size", while terms relating to mitosis and DNA replication are significantly overrepresented in the developmentally repressed genes (Table S5). Of the 237 genes induced by *br*, 147 (62.0%) were upregulated at the 0 hr stage in w^{1118} flies and only 18 (7.6%) were downregulated at the 0 hr stage (Figure 4B). In contrast with the predictions of the hierarchical model of ecdysone-driven gene regulation, more *br*-repressed genes were upregulated in 0 hr prepupae than downregulated, although the difference was not significant [126 genes and 112 genes (26.3% and 23.3%), respectively] (Figure 4B).

The absence of metabolic gene ontology terms among those enriched in the developmentally induced genes suggests that wild-type discs persist in their metabolic activity even as the larval tissues are downregulating metabolism (Merkey *et al.* 2011), and that this maintenance of metabolism is dependent upon *br* function. This notion is consistent with the observation that *br* mutant leg discs appear to arrest development at about 4 hr APF (Figure 1). To address this experimentally, we quantified ATP levels in +4 hr w^{1118} and br^5 mutant imaginal discs. To ensure sufficient sample size, we used mixed leg and wing imaginal discs. To our surprise, we found that ATP levels were significantly higher in br^5 discs ($P = 0.03$, Figure S2).

Change in br expression in imaginal discs features an isoform switch at metamorphosis

Although the large proportion of *br*-regulated genes that are temporally regulated at metamorphosis is generally consistent with the hierarchical model of *br* gene regulation, in which *br* is induced by ecdysone and in turn induces the late response genes, we also found many *br*-regulated genes that do not appear to be developmentally regulated (Figure 4B). We therefore suspected a more complex relationship between ecdysone-regulated and *br*-regulated genes. Given that previous work has shown differential expression of *br* isoforms in different tissues (Huet *et al.* 1993), we wanted to investigate the expression of *br* in imaginal discs relative to the late larval ecdysone pulse. We therefore performed a northern blot analysis using total RNA isolated from wild-type (*Binsn/Y*) leg discs at six time points from 18 hr before pupariation to 6 hr after pupariation (Figure 5A), and probed the samples for expression of all four *br* isoforms (using a probe specific to the core BTB/POZ domain) and the *br-Z2* isoform. It is noteworthy that the *br* Z2 isoform is clearly expressed in leg imaginal discs as early as 18 hr before puparium formation, and that its expression tails off just after the onset of metamorphosis and is gone by 4 hr APF. In contrast, using the *br*-core probe, we note that the *br-Z1* isoform (~4.4 kb transcript) shows minimal expression 18 hr before pupariation, and highest expression between 2 and 4 hr after pupariation in leg imaginal discs. This pattern of gene expression was confirmed with five additional imaginal disc Northern blots, four of which included both leg and wing samples, and closely matches what has been reported for whole animals at these time points (Andres and Thummel 1994).

Since transcription of the Z2 isoform of *br* appears to stop at or near the onset of metamorphosis, we suspected that derepression of some Br-repressed genes may be critical for leg morphogenesis. We therefore attempted to disrupt this process by misexpressing the *br Z2* isoform during the prepupal stage. To accomplish this, we heat shocked late larvae carrying a heat-inducible *br* Z2 construct (Crossgrove *et al.* 1996), collected all animals that pupariated within 6 hr after the heat shock, and followed the animals through prepupal and pupal development. In six separate experiments totaling 99 animals, only 50% of the *HS-brZ2* animals pupated, and of those only 4 developed to late pupae (none eclosed), with the remaining dying as early pupae (Figure 5, B and C). Most of those that pupated had short legs and wings (Figure 5B) or poorly everted heads. In contrast 98% of w^{1118} animals treated in the same way pupated ($n = 106$), and developed to late pupae (Figure 5C). In a separate experiment of 80 w^{1118} animals treated in the same way 73% eclosed (Figure 5C). Dissection of leg imaginal discs from the dead *hs-brZ2* prepupae revealed variable terminal leg phenotypes, but most appeared to arrest at stages comparable to wild-type legs between 4 and 7 hr APF (Figure 5D). To confirm that the first

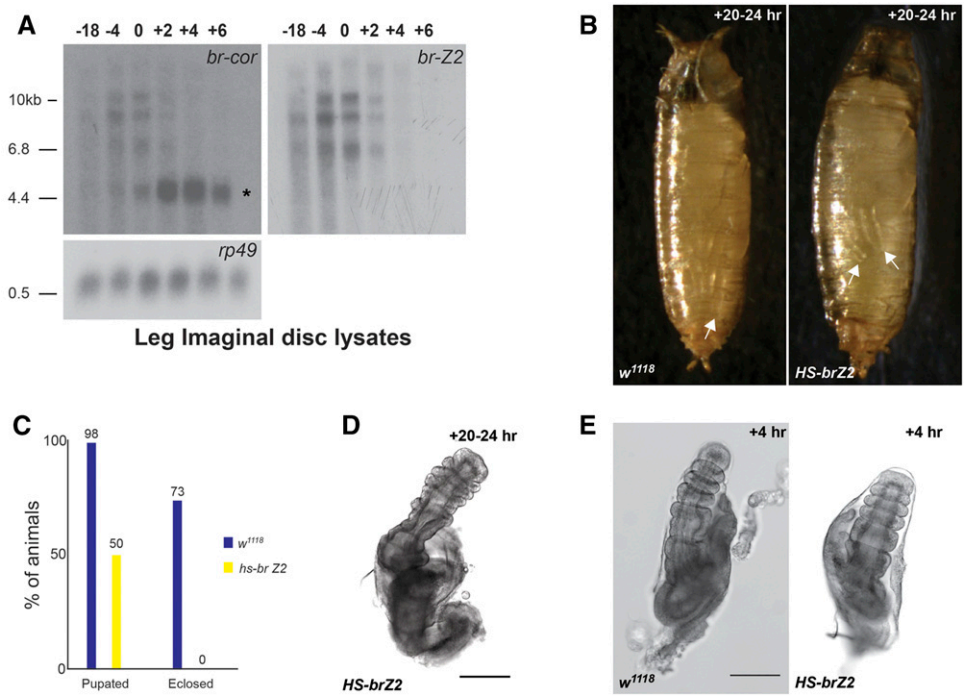

Figure 5 Downregulation of *br* expression at the onset of metamorphosis is required for normal late prepupal and pupal development. (A) Northern blot analysis of total RNA extracted from leg imaginal discs from third instar larvae (−18 hr and −4 hr relative to pupariation) and prepupae (0, +2, +4, and +6 hr) showing expression of all *br* isoforms (*br-core*) and just *br-Z2*. Expression of the *Z2* isoform is substantially reduced by 2 hr after pupariation and is absent by 4 hr after pupariation. Note that the *Z1* isoform (~4.4 kb, indicated by asterisk) is upregulated at the onset of metamorphosis (0 hr) and is strongly expressed by 2 hr after pupariation in leg discs. *rp49* was used as a control for loading and RNA transfer. (B) Photomicrographs of w^{1118} (left side) and *HS-brZ2* (right side) early pupae ~20–24 hr after pupariation that had been heat shocked at 37° for 60 min within 6 hr before pupariation. The *HS-brZ2* pupae has short legs (arrows indicate the distal tips of legs in the two animals). (C) Quantification of pupation and eclosion in w^{1118} and *hs-br Z2* animals that had been heat shocked within 6 hr of pupariation. (D) Brightfield photomicrograph of a leg disc from a *HS-brZ2* dead prepupae ~20–24 hr after pupariation that had been heat shocked at 37° for 60 min within 6 hr before pupariation. Note that this animal had not pupated and the leg disc was found inside the degenerating prepupae. This terminal phenotype is similar to what is seen in a wild-type prepupae at about 6 or 7 hr after pupariation. (E) Brightfield photomicrograph of leg discs from w^{1118} (left side) and *HS-brZ2* (right side) 4 hr after pupariation that had been heat shocked at 37° for 60 min within 6 hr before pupariation. Note that the *HS-brZ2* leg disc looks similar to that from w^{1118}. Bar, 100 μm.

several hours of prepupal development occurred normally in these animals, we repeated the experiment, collected animals as they pupariated, aged them 4 hr, and then dissected and imaged the leg imaginal discs. All the legs appeared to have elongated normally at +4 hr regardless of how many hours (0–5 hr) before pupariation that they were heat shocked (Figure 5E). Taken together, these results suggest that either the continued expression of some *br*-induced genes or failure to derepress some *br*-repressed genes are detrimental to later prepupal and pupal leg development.

Functional analysis of br-induced genes in leg morphogenesis

Given the important role that *br* plays in leg disc morphogenesis, we expected that some of the genes induced by *br* in the leg discs at metamorphosis would also be critical for this process. To test this, we induced RNAi using *Distal-less* (*Dll*)-*GAL4*. *Dll-GAL4* is expressed in the distal tibia and tarsal segments during late larval and prepupal time points (Cohen 1993; Ward *et al.* 2003). We chose *br*-target genes that fell into a number of different categories. We tested genes with "ATP generation from ADP" and "Generation of precursor metabolites and energy" gene ontology annotations. We tested genes with peptidase or peptidase inhibition functions due to our observation that basal ECM degradation is perturbed in br^5 mutant leg discs (Figure 3), and we were particularly interested in *Stubble* (*Sb*) because it has been shown in previous screens to have an enhancer of *br* effect (Beaton *et al.* 1988; Gotwals and Fristrom 1991; Ward *et al.* 2003). We tested members of the *Enhancer of split* complex due to the enrichment of the "Notch signaling" GO term among *br*-induced genes. We also tested a collection of genes that have chitin-related functions since the gene ontology enrichment showed an overrepresentation of these genes in the *br*-induced set. Finally, we also tested several genes in the Ecdysone-induced 71E cluster (Eig71E), since 6 of the 11 Eig71E genes were found to be *br*-induced.

In control experiments, we drove the expression of *br*-RNAi in distal leg segments and observed no adults; +4 hr leg discs from *Dll* > *br-RNAi* animals revealed defects similar to that observed in br^5 animals (Figure S3, B and C). Specifically, both br^5 and *Dll* > *br-RNAi* leg imaginal discs show incomplete elongation with deeper folds between segments, although discs in which *br* was knocked down via RNAi show slightly greater elongation than br^5 legs. No additional elongation was observed in *Dll* > *br-RNAi* leg discs beyond 4 hr APF (data not shown). Distal leg expression of *Sb-RNAi* resulted in 18% of the animals displaying a malformed leg phenotype characterized by shorter, fatter distal tibia and tarsal segments (Figure 6B). This malformed phenotype is similar to that observed in a hypomorphic *Sb* allele (Figure 6C). These experiments validate the use of *Dll-GAL4* to

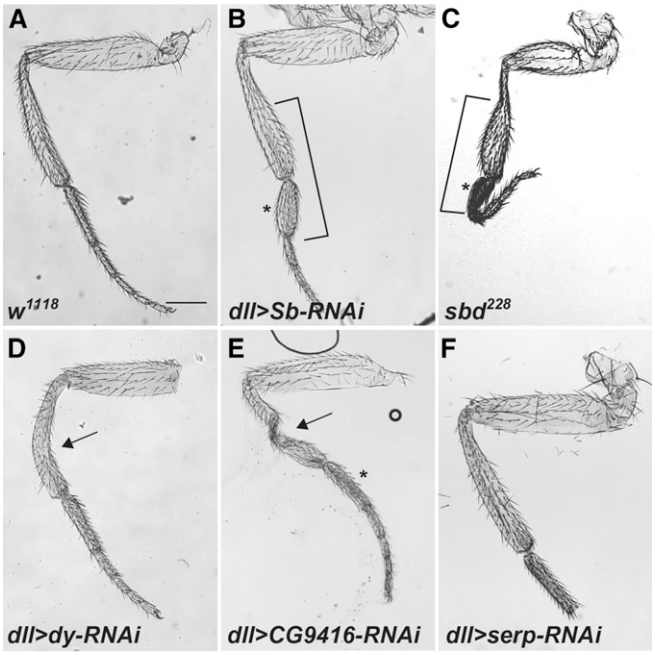

Figure 6 Driving RNAi against some *br*-induced genes in distal leg segments leads to malformed adult legs. Brightfield photomicrographs of adult legs from w^{1118} (A), *Dll* > *Sb-RNAi* (B), Sb^{Ebr228} (C), *Dll* > *dy-RNAi* (D), *Dll* > *CG9416-RNAi* (E), and *Dll* > *serp-RNAi* (F). Note that the *Dll* > *Sb-RNAi* (B) has a shorter and fatter distal tibia and tarsal segment similar to that observed in the homozygous *sbd* mutant (brackets) (C). Malformed phenotypes include bends or kinks in the tibia (arrows), and misshapen tarsal segments (asterisks). *Dll* > *serp-RNAi* flies (F) show a high penetrance of missing distal tarsal segments. Bar, 200 μm.

reduce gene expression of *br*-induced genes during late larval and prepupal leg morphogenesis.

We next drove RNAi against 36 *br*-induced genes using both long-hairpin and short-hairpin *UAS-RNAi* lines with the *Dll-GAL4* driver. A total of 41 RNAi lines were tested, and phenotypes similar to those reported in screens by Ward *et al.*, including bent tibias and poorly proportioned tarsals (Ward *et al.* 2003), were observed in several of the lines (Table 2 and Figure 6). In total, five lines exhibited malformed legs at a rate of >4%, including two lines from the protease and protease inhibitor group, *CG9416* and *Sb*, and two lines knocking down chitin-related genes, *dusky* (*dy*) and *serp*. The final line carried a construct against *grainy head* (*grh*). In all cases, straight winged flies that carried the *GAL4* driver showed significantly more leg defects than curly-winged flies from the same cross that did not carry the GAL4 driver ($P < 0.001$; Table 2). The phenotypes observed in each of these crosses differed (Figure 6): in those from the *dy* line, flies exhibited slightly curved tibias, while flies from the *CG9416* line exhibited more severely kinked tibias. *serp* line flies frequently showed bent or missing tarsal segments, while the tarsal segments in *Sb* and *grh* flies were often misshapen or misproportioned (Figure 6B and data not shown). Variation in phenotype penetrance and expressivity also existed between crosses with lines carrying constructs against the same genes (Table 2). For example, bent tibias were observed in 38% of flies expressing a short-hairpin construct against *CG9416*, while flies expressing a long-hairpin construct did not display this phenotype.

Several lines produced fewer of the straight-winged RNAi-expressing flies than expected, suggesting some lethal effect. In total, 16 crosses targeting *br*-induced genes resulted in significantly <50% of straight wing flies (Table 2). These include four crosses (*CG9416*, *grh*, *Sb*, and *serp*) that exhibited malformed legs at a rate of >4%, as well as three crosses {*vermiform* (*verm*), *Enhancer of split mα* [*E(spl)mα*], and *Glyceraldehyde 3 phosphate dehydrogenase 2* (*Gapdh2*)} that produced no RNAi-expressing straight wing flies that could be scored for the malformed leg phenotype. Individuals expressing RNAi against *E(spl)mα* failed to undergo larval molts, appearing to remain as first instar larvae for several days before dying (data not shown). In contrast, individuals expressing RNAi against *verm* or *Gapdh2* pupariated. Among offspring of the *verm* RNAi cross, the majority of the animals pupated, but without everting their legs. After about a day following pupation, there was noticeable necrotic tissue in the areas where the legs, the antennae, and wing margins form in wild-type pupae (Figure 7B). A similar phenotype was observed in offspring of the *Gapdh2* RNAi cross, but at a relatively low penetrance (data not shown). When we dissected +4 hr leg discs from *Dll* > *verm-RNAi* prepupae, we found that they exhibited an elongation defect that was more severe than what was observed in br^5 mutants or *br* RNAi knockdown flies (compare Figure 7D to Figure S3, B and C). To investigate whether the majority of the br^5 mutant phenotype is due to loss of *verm*, we drove UAS-*verm* in *br* RNAi imaginal discs (using *Dll-GAL4*). Neither expression of *verm* (nor its fellow chitin deacetylase, *serp*), was able to rescue *br* RNAi flies to adulthood (7 independent experiments with *UAS-verm* with $n = 409$ adults eclosing and 4 independent experiments with *UAS-serp* with $n = 291$ adults eclosing). We then examined the +4 hr leg imaginal discs from animals expressing *UAS-serp* in *Dll* > *br-RNAi* and found no rescue of the prepupal leg defect, although there is clear evidence of Serp expression ($n = 54$ legs from 14 animals; Figure S3).

Another metabolism gene, *Phosphoglucose mutase 1* (*Pgm1*), was of interest because only 13% of expected *Dll* > *Pgm1-RNAi* animals eclosed (Table 2), and the cytological location of Pgm1 in 72D8 on the third chromosome overlapped a br^1-interacting loci from our previous screen (Ward *et al.* 2003). We examined *Dll* > *Pgm1-RNAi* prepupae and pupae and observed that approximately 25% failed to pupate; however, those that did pupate had normal looking legs (data not shown). We then crossed flies carrying the lethal $Pgm1^{LA00593}$ allele (genotype $Pgm1^{LA00593}$/*TM3 Sb Ser*) to br^1 females and observed that 21.4% of the br^1/Y; $Pgm1^{LA00593}/+$ adults exhibited malformed legs ($n = 103$).

Discussion

In this study, we have demonstrated that Br is required for many of the tissue-level events required for leg morphogenesis

Table 2 Frequency of leg defects in flies expressing RNAi against *br*-induced genes

Target gene	TRiP or VDRC	Line no.	% Carrying *dll > Gal4*	% With malformed legs	Note
Protease and protease inhibitors					
CG3355	TRiP	52897	48.9%	0.0%	
CG5639	TRiP	57376	48.2%	0.0%	
	VDRC	1306	50.0%	1.2%	
CG8170	TRiP	61889	36.2%	0.0%	
CG9416	**TRiP**	**57563**	**28.6%**	**37.5%** ***n* = 32**	**Bent tibias; 0 out of 80 flies without *dll > Gal4* had malformed legs**
	VDRC	10064	45.9%	2.6%	
Stubble	**TRiP**	**42647**	**30.4%**	**23.0%** ***n* = 61**	**Bent femurs, tibias, and tarsals; 2 out of 159 flies without *dll > Gal4* had malformed legs**
Serine Protease Immune Response Integrator	TRiP	42882	47.1%	0.0%	
Notch pathway genes					
Enhancer of split m4	TRiP	61261	41.3%	1.5%	
Enhancer of split m7	TRiP	29327	51.6%	1.3%	
Enhancer of split m8	TRiP	26322	39.4%	1.2%	
	VDRC	37686	45.6%	0.0%	
Enhancer of split mα	VDRC	35886	0.0%	N/A	No adult flies—larvae failed to molt
Enhancer of split mγ	TRiP	51762	48.0%	0.0%	
Scabrous	TRiP	56928	54.3%	0.0%	
Eig71E genes					
Ecdysone-induced gene 71Ec	TRiP	57384	45.9%	0.0%	
Ecdysone-induced gene 71Ed	TRiP	56952	52.4%	0.0%	
Ecdysone-induced gene 71Ef	TRiP	55930	46.1%	0.0%	
Ecdysone-induced gene 71Eg	TRiP	56953	47.9%	0.9%	
Chitin-related genes					
Dusky	TRiP	34382	55.3%	0.0%	All flies had slightly curved tibias, but not severe enough to be counted as malformed
	VDRC	**3299**	**41.5%**	**100.0%** ***n* = 44**	**Bent tibias; 0 out of 62 flies without *dll > Gal4* had malformed legs**
Imaginal disc growth factor 4	TRiP	55381	45.8%	0.0%	
Serpentine	**TRiP**	**65104**	**15.4%**	**18.2%** ***n* = 35**	**Bent or broken tarsals; 0 out of 192 flies without *dll > Gal4* had malformed legs**
Vermiform	TRiP	57188	0.0%	N/A	Died as prepupae
Metabolic genes					
Aldolase 1	TRiP	65884	25.0%	0.0%	
Enolase	TRiP	26300	1.4%	0.0%	
Glyceraldehyde 3 phosphate dehydrogenase 2	TRiP	26302	0.0%	N/A	**Died as pupae/some failed to evert legs**
Glycogen phosphorylase	TRiP	33634	40.3%	1.9%	
Phosphofructokinase	TRiP	34336	46.3%	0.0%	
Phosphoglycerate kinase	TRiP	33633	43.2%	0.0%	
Phosphoglyceromutase 78	TRiP	26303	49.1%	0.9%	
Phosphoglucose mutase 1	TRiP	34345	12.9%	0.0%	
Triose phosphate isomerase	TRiP	51829	47.7%	0.0%	
Miscellaneous					
Amalgam	TRiP	33416	14.8%	0.0%	
	VDRC	22944	45.2%	0.0%	
CG5758	TRiP	57808	33.3%	0.0%	
Slowdown	VDRC	106464	45.4%	3.6%	
CG10960	TRiP	34598	45.8%	0.0%	
CG12026	VDRC	42480	42.7%	6.6%	
Grainy head	**TRiP**	**42611**	**37.8%**	**6.6%** ***n* = 106**	**Short, fat tarsals; 0 out of 175 flies without *dll > Gal4* had malformed legs**
Ecdysone-inducible gene E3	VDRC	16402	40.0%	0.0%	

Lines listed include both TRiP and VDRC (long hairpin) lines, with stock numbers shown. Lines exhibiting a significant number of malformed legs are indicated in bold. Percentages of adult flies carrying the Gal4 driver (determined by absence of curly wings) is indicated; values found by chi-square test to be significantly lower than 50% are underlined. All RNAi lines were crossed with virgin females carrying the *Dll*-Gal4 driver and a UAS-*Dicer* construct.

during the first several hours of metamorphosis in *Drosophila*, and have identified a collection of genes regulated by *br* that may help explain this developmental process. Many previous studies have demonstrated that leg morphogenesis requires ecdysone signaling (Mandaron 1971; Fristrom *et al.* 1973), cell shape changes and rearrangements (Condic *et al.* 1991), and proteolysis of the ECM (Diaz-de-la-Loza *et al.* 2018). Here, we show that leg discs in br^5 mutant animals fail to fully degrade their ECM (Figure 2), and that even if the ECM is degraded by exogenous trypsin, they fail to fully elongate (Figure 3), suggesting that the underlying cell shape changes and rearrangements are also defective. Anisometric cell shapes and wider tarsal segments in +4 hr leg discs from br^5 mutant animals support this suggestion (Figure 3). Consistent with all of these observations, RNA-sequencing comparisons between br^5 and w^{1118} leg imaginal discs at the onset of morphogenesis indicate that *br* regulates the expression of several potential proteases and chitin-modifying genes. RNAi-based functional analyses confirm a requirement for some of these *br*-induced genes in leg imaginal disc morphogenesis (Figures 6 and 7). Furthermore, bioinformatic analyses of *br*-regulated genes suggests that *br* is required to maintain robust metabolism in imaginal discs when glycolysis is otherwise downregulated in the larval tissues.

br-dependent ECM remodeling plays a critical role in leg development

Our results suggest that *br* plays a central role in remodeling the ECM in leg imaginal discs during metamorphosis. We show that Collagen IV is not cleared from the basal ECM in br^5 mutant prepupal leg discs (see Figure 2). In addition, four of the six genes that resulted in malformed adult legs when downregulated by RNAi (*dusky*, *serpentine*, *Stubble*, and *vermiform*) have been proposed to interact with the apical ECM, while another (*grainy head*) is known to regulate ECM genes (Pare *et al.* 2012; Yao *et al.* 2017). *Stubble* encodes a serine protease whose endopeptidase domain is required for normal leg development (Appel *et al.* 1993; Hammonds and Fristrom 2006). Stubble protein has been shown to be required for degradation of the Dumpy protein, an apical ECM component that links the epithelial cells to the cuticle (Diaz-de-la-Loza *et al.* 2018). In the absence of this degradation, imaginal discs fail to elongate. *serpentine* and *vermiform* were identified as genes encoding chitin deacetylases involved in organization of the larval tracheal apical ECM (Luschnig *et al.* 2006). These genes are also found in the larval cuticle, where they are apically secreted and necessary for the formation of a stable matrix (Pesch *et al.* 2015; Pesch *et al.* 2016). The *dusky* gene encodes a zona pellucida protein that is expressed in epithelial tissues across *Drosophila* development, most notably in the developing wing disc during wing elongation (Roch *et al.* 2003; Jazwinska and Affolter 2004; Ren *et al.* 2005). Zona pellucida proteins are membrane-anchored proteins that interact with the ECM; a study of embryonic denticles showed localization to specific apical subcellular domains, where the proteins organize and modify the ECM to control cell shape changes (Fernandes *et al.* 2010). *grainy head* encodes a transcription factor that regulates genes involved in cuticle formation (Bray *et al.* 1989; Dynlacht *et al.* 1989; Bray and Kafatos 1991). *grainy head* mutants display defective ECM phenotypes in the head skeleton (Nusslein-Volhard *et al.* 1984; Bray and Kafatos 1991), trachea (Hemphala *et al.* 2003), and in wound repair (Mace *et al.* 2005). Chromatin immunoprecipitation data suggests that Grainy head also regulates some of the other leg morphogenesis genes identified in this study, including *CG9416*, *serpentine*, *vermiform*, and *Stubble* (Pare *et al.* 2012; Yao *et al.* 2017).

The connection that most of these genes have with the ECM is consistent with the known role of the ECM in imaginal disc elongation; the ECM provides a constraining force to imaginal discs (Pastor-Pareja and Xu 2011), and both the apical and basal ECMs must be degraded before elongation (Diaz-de-la-Loza *et al.* 2018). Our results suggest that *br* provides a key regulatory mechanism for these processes, and that they underlie a large part of the br^5 phenotype. *br* does not appear to be wholly responsible for the proteolysis of the ECM at metamorphosis, however. Notably absent from our list of *br*-regulated genes are the matrix metalloprotease genes *Mmp1* and *Mmp2*, which are required for breakdown of the basal ECM during disc eversion (Srivastava *et al.* 2007), although both of these genes are developmentally upregulated at the onset of metamorphosis in leg discs (Table S4).

Br appears to play a role in maintaining metabolic activity during metamorphosis

The amorphic br^5 allele leads to failure of imaginal disc development, and, as expected, several development-related biological process gene ontology terms were enriched in *br*-induced genes, including "developmental process," "anatomical structure development," and "organ morphogenesis." Somewhat surprisingly, the enriched gene ontology terms also included glycolysis-related metabolic terms, including "pyruvate metabolic process," "ATP generation from ADP," and "glycolytic process." In support of these findings, KEGG pathway analysis identified glycolysis/gluconeogenesis as the most significantly enriched pathway from these genes. More interestingly, neither analysis revealed enrichment of glycolysis-related metabolic genes in the comparison of w^{1118} leg discs from −18 to 0 hr (neither up- nor downregulated at 0 hr). This finding contrasts with previous microarray studies in both *D. melanogaster* and the silkworm *Bombyx mori* showing downregulation of glycolytic and other metabolic genes in whole animals at pupariation (White *et al.* 1999; Tian *et al.* 2010). Taken together, these results suggest that while larval tissues are shutting down metabolism (Merkey *et al.* 2011), the imaginal discs retain metabolic activity throughout the transition to prepupa, and that this metabolic program requires Br. This energy requirement could be needed for the cell shape changes and rearrangements that drive leg morphogenesis. Consistent with this idea, knockdown of the glycolysis gene *Gapdh2* results in failure of leg discs to elongate

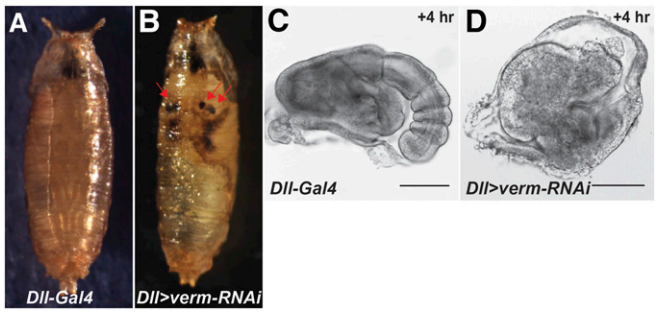

Figure 7 Distal leg expression of *verm-RNAi* leads to severe defects in leg morphogenesis. (A and B) Color photomicrographs of *Dll-Gal4* (A) and *Dll* > *verm-RNAi* (B) midstage pupae. Note the lack of elongated legs in the *Dll* > *verm-RNAi* animal that instead shows necrotic tissue in the areas where the legs should evert from (arrows). (C and D) Brightfield photomicrographs of leg imaginal disc from *Dll-Gal4* (C) and *Dll* > *verm-RNAi* (D) +4 hr prepupae showing little distal elongation and almost no segmentation in the *verm-RNAi* disc. Bar, 100 μm.

and evert in some pupae, and knockdown of any of four other metabolism genes appears to result in larval or pupal lethality (Table 2). One of these genes, *Phosphoglucose mutase 1* also dominantly enhanced the malformed leg phenotype associated with br^1, similar to what we previously observed with the overlapping deficiency *Df(3L)brm11* (Ward *et al.* 2003). Given these observations, we were surprised to find ATP levels were higher in br^5 mutant discs than in w^{1118} discs at 4 hr after pupariation (Figure S2), but this result may instead reflect the reduced energy consumption of br^5 mutant leg discs that have already arrested morphogenesis by 4 hr APF.

broad is dynamically regulated before and during metamorphosis

The *Broad-Complex* was initially described as an early-response gene in the ecdysone-induced transcriptional cascade (Chao and Guild 1986; DiBello *et al.* 1991), but subsequent experiments suggested that the regulation of *br* by ecdysone both in whole animals and in imaginal discs is more complex and involves an isoform switch from *Z2* to *Z1* at pupariation. Specifically, studies in the salivary glands and whole animals showed a switch to *Z1* upon pupariation (Andres *et al.* 1993; Huet *et al.* 1993), and imaginal discs cultured in the presence of ecdysone resulted in persistence of the *Z1* transcript even after the other *br* isoforms were no longer detected (Bayer *et al.* 1996). Our Northern blot analysis confirms this isoform switch at the onset of metamorphosis in imaginal discs, and also reveals that *br Z2* is expressed earlier in the discs than would be predicted by whole animal blots (Figure 5A; Andres and Thummel 1994). This latter observation is somewhat paradoxical considering that the *br*-induced genes are a reasonably good subset of the developmentally induced genes revealed by RNA-sequencing comparisons of leg discs from −18 to 0 hr (Figure 4). This raises the possibility that many of these *br*-induced genes are also regulated in a temporal fashion, perhaps by ecdysone/EcR/Usp directly. Future experiments should be aimed at exploring the more complex regulation of these genes, particularly those that we have identified as playing important roles in driving leg morphogenesis. It is also interesting that Br appears to be responsible for controlling early prepupal developmental events (proteolysis of the ECM, cell shape changes and rearrangements) when the Z2 isoform is ostensibly "off." We believe that this is driven by perdurance of the Br protein. In support of this, Emery *et al.* (1994) demonstrated that levels of the Br-Z2 protein remained strong in the imaginal discs until between 4 and 8 hr after pupariation, despite the decrease in transcription by 0 hr. Finally, it is worth noting that we identified a large number of *br*-repressed genes in our RNA-sequencing experiment, raising the possibility that derepression of *br*-repressed genes may also contribute to normal leg morphogenesis. Our functional studies, in which we extended *br-Z2* expression through a heat-inducible promoter, resulted in complete lethality, with half of the animals dying prior to pupation. The terminal leg phenotypes in the prepupal lethal animals revealed that development was normal until 4–7 hr after pupariation. For those animals that pupated, their legs and wings were short, the heads were often malformed, and they died soon after pupation. Taken together, these findings are consistent with a model in which perdurance of Br is sufficient to positively regulate genes needed for early prepupal leg development, at which point reduced Br results in derepression of a second set of genes that positively affects later prepupal and pupal leg development.

Acknowledgments

We thank Stefan Luschnig, Christos Samakovlis, Cindy Bayer, Sally Horne-Badovinac, the Bloomington *Drosophila* Stock Center, and the Vienna *Drosophila* RNAi Center for fly stocks, and Stefan Luschnig for the anti-Verm antibody. We thank Taybor Parker, David Davido, and Rob Unckless for help with the ATP measurement and analysis. The DCAD2 antibody developed by T. Uemura was obtained from the Developmental Studies Hybridoma Bank, created by the National Institute of Child Health and Human Development of the National Institutes of Health and maintained at The University of Iowa, Department of Biology, Iowa City, IA. We also thank Rebecca Spokony, Laurie von Kalm, Jason Tennessen, and members of the Ward laboratory for helpful discussion about the project and manuscript. This work was supported by the College of Liberal Arts and Sciences at the University of Kansas (to C.R.). RNA-sequencing was supported by a University of Kansas genome sequencing core users grant (to R.E.W.). The sequencing core is supported by National Institutes of Health grant P20-GM-103638 (Susan Lunte, PI). Analysis of RNA-sequencing data (by S.J.M.) was aided by infrastructure purchased via the Kansas IDeA Network of Biomedical Research Excellence (National Institutes of Health grant P20-GM-103418). The funders had no role in study design, data collection and analysis, decision to publish, or preparation of the manuscript. The authors have declared that no competing interests exist.

Literature Cited

Andres, A. J., and C. S. Thummel, 1994 Methods for quantitative analysis of transcription in larvae and prepupae, pp. 565–573 in *Drosophila melanogaster: Practical Uses in Cell and Molecular Biology*, edited by L. Goldstein and E. Fryberg. Academic Press, Cambridge, MA.

Andres, A. J., J. C. Fletcher, F. D. Karim, and C. S. Thummel, 1993 Molecular analysis of the initiation of insect metamorphosis: a comparative study of *Drosophila* ecdysteroid-regulated transcription. Dev. Biol. 160: 388–404.

Andrews, S., 2010 FastQC: a quality control tool for high throughput sequence data [Online].

Appel, L. F., M. Prout, R. Abu-Shumays, A. Hammonds, J. C. Garbe *et al*., 1993 The *Drosophila Stubble-stubbloid* gene encodes an apparent transmembrane serine protease required for epithelial morphogenesis. Proc. Natl. Acad. Sci. USA 90: 4937–4941.

Bassett, M. H., J. L. McCarthy, M. R. Waterman, and T. J. Sliter, 1997 Sequence and developmental expression of *Cyp18*, a member of a new cytochrome P450 family from *Drosophila*. Mol. Cell. Endocrinol. 131: 39–49.

Bayer, C. A., B. Holley, and J. W. Fristrom, 1996 A switch in *Broad-Complex* zinc-finger isoform expression is regulated post-transcriptionally during the metamorphosis of *Drosophila* imaginal discs. Dev. Biol. 177: 1–14.

Bayer, C. A., L. von Kalm, and J. W. Fristrom, 1997 Relationships between protein isoforms and genetic functions demonstrate functional redundancy at the *Broad-Complex* during *Drosophila* metamorphosis. Dev. Biol. 187: 267–282.

Beaton, A. H., I. Kiss, D. Fristrom, and J. W. Fristrom, 1988 Interaction of the *Stubble-stubbloid* locus and the *Broad-Complex* of *Drosophila melanogaster*. Genetics 120: 453–464.

Bolger, A. M., M. Lohse, and B. Usadel, 2014 Trimmomatic: a flexible trimmer for Illumina sequence data. Bioinformatics 30: 2114–2120.

Bray, S. J., and F. C. Kafatos, 1991 Developmental function of Elf-1: an essential transcription factor during embryogenesis in *Drosophila*. Genes Dev. 5: 1672–1683.

Bray, S. J., B. Burke, N. H. Brown, and J. Hirsh, 1989 Embryonic expression pattern of a family of *Drosophila* proteins that interact with a central nervous system regulatory element. Genes Dev. 3: 1130–1145.

Burtis, K. C., C. S. Thummel, C. W. Jones, F. D. Karim, and D. S. Hogness, 1990 The *Drosophila* 74EF early puff contains *E74*, a complex ecdysone-inducible gene that encodes two ets-related proteins. Cell 61: 85–99.

Buszczak, M., S. Paterno, D. Lighthouse, J. Bachman, J. Planck *et al*., 2007 The Carnegie Protein Trap Library: a versatile tool for *Drosophila* developmental studies. Genetics 175: 1505–1531.

Chao, A. T., and G. M. Guild, 1986 Molecular analysis of the ecdysterone-inducible 2B5 "early" puff in *Drosophila melanogaster*. EMBO J. 5: 143–150.

Cohen, S. M., 1993 Imaginal disc development, pp. 747–841 in *The Development of Drosophila melanogaster*, edited by M. Bate and A. Martinez Arias. Cold Spring Harbor Laboratory Press, Cold Spring Harbor, NY.

Condic, M. L., D. Fristrom, and J. W. Fristrom, 1991 Apical cell shape changes during *Drosophila* imaginal leg disc elongation: a novel morphogenetic mechanism. Development 111: 23–33.

Crossgrove, K., C. A. Bayer, J. W. Fristrom, and G. M. Guild, 1996 The *Drosophila Broad-Complex* early gene directly regulates late gene transcription during the ecdysone-induced puffing cascade. Dev. Biol. 180: 745–758.

Csaba, G., 1977 Hormonal regulation: morphogenetic and adaptive systems. Biol. Rev. Camb. Philos. Soc. 52: 295–303.

De las Heras, J. M., C. Garcia-Cortes, D. Foronda, J. C. Pastor-Pareja, L. S. Shashidhara *et al*., 2018 The *Drosophila* Hox gene *Ultrabithorax* controls appendage shape by regulating extracellular matrix dynamics. Development 145: dev161844. https://doi.org/10.1242/dev.161844

Diaz-de-la-Loza, M., R. P. Ray, P. S. Ganguly, S. Alt, J. R. Davis *et al*., 2018 Apical and basal matrix remodeling control epithelial morphogenesis. Dev. Cell 46: 23–39.

DiBello, P. R., D. A. Withers, C. A. Bayer, J. W. Fristrom, and G. M. Guild, 1991 The *Drosophila* Broad-Complex encodes a family of related proteins containing zinc fingers. Genetics 129: 385–397.

Dietzl, G., D. Chen, F. Schnorrer, K. C. Su, Y. Barinova *et al*., 2007 A genome-wide transgenic RNAi library for conditional gene inactivation in Drosophila. Nature 448: 151–156.

Dynlacht, B. D., L. D. Attardi, A. Admon, M. Freeman, and R. Tjian, 1989 Functional analysis of NTF-1, a developmentally regulated *Drosophila* transcription factor that binds neuronal *cis* elements. Genes Dev. 3: 1677–1688.

Emery, I. F., V. Bedian, and G. M. Guild, 1994 Differential expression of *Broad-Complex* transcription factors may forecast tissue-specific developmental fates during *Drosophila* metamorphosis. Development 120: 3275–3287.

Feigl, G., M. Gram, and O. Pongs, 1989 A member of the steroid hormone receptor gene family is expressed in the 20-OH-ecdysone inducible puff 75B in *Drosophila melanogaster*. Nucleic Acids Res. 17: 7167–7178.

Fernandes, I., H. Chanut-Delalande, P. Ferrer, Y. Latapie, L. Waltzer *et al*., 2010 Zona pellucida domain proteins remodel the apical compartment for localized cell shape changes. Dev. Cell 18: 64–76.

Fristrom, D., 1988 The cellular basis of epithelial morphogenesis: a review. Tissue Cell 20: 645–690.

Fristrom, J. W., W. R. Logan, and C. Murphy, 1973 The synthetic and minimal culture requirements for evagination of imaginal discs of *Drosophila melanogaster in virtro*. Dev. Biol. 33: 441–456.

Gatti, M., and B. S. Baker, 1989 Genes controlling essential cell-cycle functions in *Drosophila melanogaster*. Genes Dev. 3: 438–453.

Gene Ontology Consortium, 2015 Gene Ontology Consortium: going forward. Nucleic Acids Res. 43: D1049–D1056.

Gotwals, P. J., and J. W. Fristrom, 1991 Three neighboring genes interact with the *Broad-Complex* and the *Stubble-stubbloid* locus to affect imaginal disc morphogenesis in *Drosophila*. Genetics 127: 747–759.

Goujon, M., H. McWilliam, W. Li, F. Valentin, S. Squizzato *et al*., 2010 A new bioinformatics analysis tools framework at EMBL-EBI. Nucleic Acids Res. 38: W695–W699.

Hammonds, A. S., and J. W. Fristrom, 2006 Mutational analysis of *Stubble-stubbloid* gene structure and function in *Drosophila* leg and bristle morphogenesis. Genetics 172: 1577–1593.

Hemphala, J., A. Uv, R. Cantera, S. Bray, and C. Samakovlis, 2003 Grainy head controls apical membrane growth and tube elongation in response to Branchless/FGF signalling. Development 130: 249–258.

Hock, T., T. Cottrill, J. Keegan, and D. Garza, 2000 The *E23* early gene of *Drosophila* encodes an ecdysone-inducible ATP-binding cassette transporter capable of repressing ecdysone-mediated gene activation. Proc. Natl. Acad. Sci. USA 97: 9519–9524.

Huet, F., C. Ruiz, and G. Richards, 1993 Puffs and PCR: the in vivo dynamics of early gene expression during ecdysone responses in *Drosophila*. Development 118: 613–627.

Hurban, P., and C. S. Thummel, 1993 Isolation and characterization of fifteen ecdysone-inducible *Drosophila* genes reveal unexpected complexities in ecdysone regulation. Mol. Cell. Biol. 13: 7101–7111.

Janknecht, R., W. Taube, H. J. Ludecke, and O. Pongs, 1989 Characterization of a putative transcription factor gene expressed in the 20-OH-ecdysone inducible puff 74EF in *Drosophila melanogaster*. Nucleic Acids Res. 17: 4455–4464.

Jazwinska, A., and M. Affolter, 2004 A family of genes encoding zona pellucida (ZP) domain proteins is expressed in various epithelial tissues during *Drosophila* embryogenesis. Gene Expr. Patterns 4: 413–421.

Karim, F. D., and C. S. Thummel, 1991 Ecdysone coordinates the timing and amounts of E74A and E74B transcription in *Drosophila*. Genes Dev. 5: 1067–1079.

Kim, D., G. Pertea, C. Trapnell, H. Pimentel, R. Kelley *et al.*, 2013 TopHat2: accurate alignment of transcriptomes in the presence of insertions, deletions and gene fusions. Genome Biol. 14: R36.

Kiss, I., A. H. Beaton, J. Tardiff, D. Fristrom, and J. W. Fristrom, 1988 Interactions and developmental effects of mutations in the *Broad-Complex* of *Drosophila melanogaster*. Genetics 118: 247–259.

Le, T., Z. Liang, H. Patel, M. H. Yu, G. Sivasubramaniam *et al.*, 2006 A new family of *Drosophila* balancer chromosomes with a *w- dfd*-GMR yellow fluorescent protein marker. Genetics 174: 2255–2257.

Luschnig, S., T. Batz, K. Armbruster, and M. A. Krasnow, 2006 *Serpentine* and *vermiform* encode matrix proteins with chitin binding and deacetylation domains that limit tracheal tube length in *Drosophila*. Curr. Biol. 16: 186–194.

Mace, K. A., J. C. Pearson, and W. McGinnis, 2005 An epidermal barrier wound repair pathway in *Drosophila* is mediated by *grainy head*. Science 308: 381–385.

Mandaron, P., 1971 Developpement *in vitro* des disques imaginaux de la Drosophile. Aspects morphologiques et histologiques. Dev. Biol. 22: 298–320.

Merkey, A. B., C. K. Wong, D. K. Hoshizaki, and A. G. Gibbs, 2011 Energetics of metamorphosis in *Drosophila melanogaster*. J. Insect Physiol. 57: 1437–1445.

Nusslein-Volhard, C., E. Wieschaus, and H. Kluding, 1984 Mutations affecting the pattern of the larval cuticle in *Drosophila melanogaster*: I. Zygotic loci on the second chromosome. Rouxs Arch. Dev. Biol. 193: 267–282.

Pare, A., M. Kim, M. T. Juarez, S. Brody, and W. McGinnis, 2012 The functions of Grainy head-like proteins in animals and fungi and the evolution of apical extracellular barriers. PLoS One 7: e36254.

Pastor-Pareja, J. C., and T. Xu, 2011 Shaping cells and organs in *Drosophila* by opposing roles of fat body-secreted Collagen IV and Perlecan. Dev. Cell 21: 245–256.

Pesch, Y., D. Riedel, and M. Behr, 2015 Obstructor A organizes matrix assembly at the apical cell surface to promote enzymatic cuticle maturation in *Drosophila*. J. Biol. Chem. 290: 10071–10082.

Pesch, Y., D. Riedel, K. R. Patil, G. Loch, and M. Behr, 2016 Chitinases and Imaginal disc growth factors organize the extracellular matrix formation at barrier tissues in insects. Sci. Rep. 6: 18340.

Proag, A., B. Monier, and M. Suzanne, 2019 Physical and functional cell-matrix uncoupling in a develping tissue under tension. Development 146: dev172577.

Ren, N., C. Zhu, H. Lee, and P. A. Adler, 2005 Gene expression during *Drosophila* wing morphogenesis and differentiation. Genetics 171: 625–638.

Roberts, A., C. Trapnell, J. Donaghey, J. L. Rinn, and L. Pachter, 2011 Improving RNA-Seq expression estimates by correcting for fragment bias. Genome Biol. 12: R22.

Roch, F., C. R. Alonso, and M. Akam, 2003 *Drosophila miniature* and *dusky* encode ZP proteins required for cytoskeletal reorganisation during wing morphogenesis. J. Cell Sci. 116: 1199–1207.

Segraves, W. A., and D. S. Hogness, 1990 The *E75* ecdysone-inducible gene responsible for the 75B early puff in *Drosophila* encodes two new members of the steroid receptor superfamily. Genes Dev. 4: 204–219.

Sievers, F., A. Wilm, D. Dineen, T. J. Gibson, K. Karplus *et al.*, 2011 Fast, scalable generation of high-quality protein multiple sequence alignments using Clustal Omega. Mol. Syst. Biol. 7: 539.

Srivastava, A., J. C. Pastor-Pareja, T. Igaki, R. Pagliarini, and T. Xu, 2007 Basement membrane remodeling is essential for *Drosophila* disc eversion and tumor invation. Proc. Natl. Acad. Sci. USA 1004: 2721–2726.

Thurmond, J., J. L. Goodman, V. B. Strelets, H. Attrill, L. S. Gramates *et al.*, 2019 Flybase 2.0: the next generation. Nucleic Acids Res. 47: D759–D765.

Tian, L., E. Guo, S. Wang, S. Liu, R. Jiang *et al.*, 2010 Developmental regulation of glycolysis by 20-hydroxyecdysone and juvenile hormone in fat body tissues of the silkworm, *Bombyx mori*. J. Mol. Cell Biol. 2: 255–263.

Trapnell, C., L. Pachter, and S. L. Salzbert, 2009 TopHat: discovering splice junctions with RNA-seq. Bioinformatics 25: 1105–1111.

Trapnell, C., B. A. Williams, G. Pertea, A. Mortazavi, G. Kwan *et al.*, 2010 Transcript assembly and quantification by RNA-seq reveals unannotated transcripts and isoform switching during cell differentiation. Nat. Biotechnol. 28: 511–515.

Trapnell, C., D. G. Hendrickson, M. Sauvageau, L. Goff, J. L. Rinn *et al.*, 2013 Differential analysis of gene regulation at transcript resolution with RNA-seq. Nat. Biotechnol. 31: 46–53.

von Kalm, L., K. Crossgrove, D. Von Seggern, G. M. Guild, and S. K. Beckendorf, 1994 The *Broad-Complex* directly controls a tissue-specific response to the steroid hormone ecdysone at the onset of *Drosophila* metamorphosis. EMBO J. 13: 3505–3516.

Wang, J., S. Vasaikar, Z. Shi, M. Greer, and B. Zhang, 2017 WebGestalt 2017: a more comprehensive, powerful, flexible and interactive gene set enrichment analysis toolkit. Nucleic Acids Res. 45: W130–W137.

Ward, R. E., J. Evans, and C. S. Thummel, 2003 Genetic modifier screens in *Drosophila* demonstrate a role for Rho1 signaling in ecdysone-triggered imaginal disc morphogenesis. Genetics 165: 1397–1415.

White, K. P., S. A. Rifkin, P. Hurban, and D. S. Hogness, 1999 Microarray analysis of *Drosophila* development during metamorphosis. Science 286: 2179–2184.

Willis, J. H., 1974 Morphogenetic action of insect hormones. Annu. Rev. Entomol. 19: 97–115.

Yao, T. P., B. M. Forman, Z. Jiang, L. Cherbas, J. D. Chen *et al.*, 1993 Functional ecdysone receptor is the product of *EcR* and *Ultraspiracle* genes. Nature 366: 476–479.

Yao, L., S. Wang, J. O. Westholm, Q. Dai, R. Matsuda *et al.*, 2017 Genome-wide identification of Grainy head targets in *Drosophila* reveals interactions with the POU domain transcription factor Vvl. Development 144: 3145–3155.

Communicating editor: D. Greenstein